10 kHz accuracy of an optical frequency reference based on $^{12}C_2H_2$-filled large-core kagome photonic crystal fibers

Kevin Knabe,[1] Shun Wu,[1] Jinkang Lim,[1] Karl A. Tillman,[1] Philip S. Light,[2] Francois Couny,[2] Natalie Wheeler,[2] Rajesh Thapa,[1] Andrew M. Jones,[1] Jeffrey W. Nicholson,[3] Brian R. Washburn,[1] Fetah Benabid,[2] and Kristan L. Corwin[1,*]

[1]Kansas State University, 116 Cardwell Hall, Manhattan, KS 66506 USA
[2]Centre for Photonics and Photonic Materials, Dept. of Physics, University of Bath, BA2 7AY, UK
[3]OFS Labs, Somerset, NJ 08873 USA
*corwin@phys.ksu.edu

Abstract: Saturated absorption spectroscopy reveals the narrowest features so far in molecular gas-filled hollow-core photonic crystal fiber. The 48-68 µm core diameter of the kagome-structured fiber used here allows for 8 MHz full-width half-maximum sub-Doppler features, and its wavelength-insensitive transmission is suitable for high-accuracy frequency measurements. A fiber laser is locked to the $^{12}C_2H_2$ $v_1 + v_3$ P(13) transition inside kagome fiber, and compared with frequency combs based on both a carbon nanotube fiber laser and a Cr:forsterite laser, each of which are referenced to a GPS-disciplined Rb oscillator. The absolute frequency of the measured line center agrees with those measured in power build-up cavities to within 9.3 kHz (1 σ error), and the fractional frequency instability is less than 1.2×10^{-11} at 1 s averaging time.

©2009 Optical Society of America

OCIS codes: (300.6460) Spectroscopy, saturation; (060.2310) Fiber optics; (120.3930) Metrological Instrumentation;

References and links

1. A. Czajkowski, A. A. Madej, and P. Dube, "Development and study of a 1.5 µm optical frequency standard referenced to the P(16) saturated absorption line in the $v_1 + v_3$ overtone band of $^{13}C_2H_2$," Opt. Commun. **234**(1-6), 259–268 (2004).
2. M. de Labachelerie, K. Nakagawa, and M. Ohtsu, "Ultranarrow $^{13}C_2H_2$ Saturated-Absorption Lines at 1.5 µm," Opt. Lett. **19**(11), 840–842 (1994).
3. C. S. Edwards, H. S. Margolis, G. P. Barwood, S. N. Lea, P. Gill, and W. R. C. Rowley, "High-accuracy frequency atlas of $^{13}C_2H_2$ in the 1.5 µm region," Appl. Phys. B **80**(8), 977–983 (2005).
4. A. A. Madej, J. E. Bernard, A. J. Alcock, A. Czajkowski, and S. Chepurov, "Accurate absolute frequencies of the $v_1 + v_3$ band of $^{13}C_2H_2$ determined using an infrared mode-locked Cr: YAG laser frequency comb," J. Opt. Soc. Am. B **23**(4), 741–749 (2006).
5. H. S. Moon, W. K. Lee, and H. S. Suh, "Absolute-frequency measurement of an acetylene-stabilized laser locked to the P(16) transition of $^{13}C_2H_2$ using an optical-frequency comb," IEEE Trans. Instrum. Meas. **56**(2), 509–512 (2007).
6. M. Musha, Y. Tamura, K. Nakagawa, and K. Ueda, "Practical optical frequency measurement system around 1.5 µm based on an acetylene-stabilized laser-locked optical frequency comb," Opt. Commun. **272**(1), 211–216 (2007).
7. P. Balling, M. Fischer, P. Kubina, and R. Holzwarth, "Absolute frequency measurement of wavelength standard at 1542nm: acetylene stabilized DFB laser," Opt. Express **13**(23), 9196–9201 (2005).
8. W. C. Swann, and S. L. Gilbert, "Pressure-induced shift and broadening of 1510-1540 nm acetylene wavelength calibration lines," J. Opt. Soc. Am. B **17**(7), 1263–1270 (2000).
9. A. M. Cubillas, J. Hald, and J. C. Petersen, "High resolution spectroscopy of ammonia in a hollow-core fiber," Opt. Express **16**(6), 3976–3985 (2008).
10. S. Ghosh, A. R. Bhagwat, C. K. Renshaw, S. Goh, A. L. Gaeta, and B. J. Kirby, "Low-light-level optical interactions with rubidium vapor in a photonic band-gap fiber," Phys. Rev. Lett. **97**(2), 023603 (2006).
11. J. Hald, J. C. Petersen, and J. Henningsen, "Saturated optical absorption by slow molecules in hollow-core photonic band-gap fibers," Phys. Rev. Lett. **98**(21), 213902 (2007).

12. K. Knabe, J. Lim, K. Tillman, R. Thapa, F. Couny, P. S. Light, J. W. Nicholson, B. R. Washburn, F. Benabid, and K. L. Corwin, "Stability of an Acetylene Frequency Reference inside Kagome Structured Hollow-Core Photonic Crystal Fiber," in *Proceedings of CLEO CWB5* (2009).
13. P. S. Light, F. Benabid, F. Couny, M. Maric, and A. N. Luiten, "Electromagnetically induced transparency in Rb-filled coated hollow-core photonic crystal fiber," Opt. Lett. **32**(10), 1323–1325 (2007).
14. F. Benabid, F. Couny, J. C. Knight, T. A. Birks, and P. S. J. Russell, "Compact, stable and efficient all-fibre gas cells using hollow-core photonic crystal fibres," Nature **434**(7032), 488–491 (2005).
15. A. R. Bhagwat, and A. L. Gaeta, "Nonlinear optics in hollow-core photonic bandgap fibers," Opt. Express **16**(7), 5035–5047 (2008).
16. F. Benabid, J. C. Knight, G. Antonopoulos, and P. S. J. Russell, "Stimulated Raman scattering in hydrogen-filled hollow-core photonic crystal fiber," Science **298**(5592), 399–402 (2002).
17. Crystal Fibre A/S, http://www.crystal-fibre.com/.
18. R. Thapa, K. Knabe, M. Faheem, A. Naweed, O. L. Weaver, and K. L. Corwin, "Saturated absorption spectroscopy of acetylene gas inside large-core photonic bandgap fiber," Opt. Lett. **31**(16), 2489–2491 (2006).
19. F. Couny, F. Benabid, and P. S. Light, "Large-pitch kagome-structured hollow-core photonic crystal fiber," Opt. Lett. **31**(24), 3574–3576 (2006).
20. G. Bjorklund, M. Levenson, W. Lenth, and C. Ortiz, "Frequency Modulation (FM) Spectroscopy," Appl. Phys. B **32**(3), 145–152 (1983).
21. R. W. P. Drever, J. L. Hall, F. V. Kowalski, J. Hough, G. M. Ford, A. J. Munley, and H. Ward, "Laser phase and frequency stabilization using an optical-resonator," Appl. Phys. B **31**(2), 97–105 (1983).
22. J. L. Hall, L. Hollberg, T. Baer, and H. G. Robinson, "Optical Heterodyne Saturation Spectroscopy," Appl. Phys. Lett. **39**(9), 680–682 (1981).
23. J. Lim, K. Knabe, K. A. Tillman, W. Neely, Y. Wang, R. Amezcua-Correa, F. Couny, P. S. Light, F. Benabid, J. C. Knight, K. L. Corwin, J. W. Nicholson, and B. R. Washburn, "A phase-stabilized carbon nanotube fiber laser frequency comb," Opt. Express **17**(16), 14115–14120 (2009).
24. Y. Wang, J. Lim, R. Amezcua-Correa, J. C. Knight, and B. R. Washburn, "Sub-33 fs Pulses from an All-Fiber Parabolic Amplifier Employing Hollow-Core Photonic Bandgap Fiber," in *Proceedings of Frontiers In Optics FWF5* (2008).
25. P. T. Systems, http://www.ptsyst.com/.
26. S. T. Dawkins, J. J. McFerran, and A. N. Luiten, "Considerations on the measurement of the stability of oscillators with frequency counters," IEEE Trans. Ultra. Ferr. Freq. Contr. **54**(5), 918–925 (2007).
27. J. Rutman, "Characterization of Phase and Frequency Instabilities in Precision Frequency Sources: Fifteen Years of Progress," in *Proceeding of the IEEE* (Institute of Electrical and Electronics Engineers, New York, 1968), pp. 1048–1075.
28. K. A. Tillman, R. Thapa, B. R. Washburn, and K. L. Corwin, "Significant Carrier Envelope Offset Frequency Linewidth Narrowing in a Prism-Based Cr:Forsterite Frequency Comb " in *Proceedings of CLEO CTuC5* (2009).
29. L. S. Ma, Z. Y. Bi, A. Bartels, K. Kim, L. Robertsson, M. Zucco, R. S. Windeler, G. Wilpers, C. Oates, L. Hollberg, and S. A. Diddams, "Frequency uncertainty for optically referenced femtosecond laser frequency combs," IEEE J. Quantum Electron. **43**(2), 139–146 (2007).
30. C. S. Edwards, G. P. Barwood, H. S. Margolis, P. Gill, and W. R. C. Rowley, "High-precision frequency measurements of the $v_1 + v_3$ combination band of $^{12}C_2H_2$ in the 1.5 µm region," J. Mol. Spectrosc. **234**(1), 143–148 (2005).
31. A. A. Madej, A. J. Alcock, A. Czajkowski, J. E. Bernard, and S. Chepurov, "Accurate absolute reference frequencies from 1511 to 1545 nm of the $v_1 + v_3$ band of $^{12}C_2H_2$ determined with laser frequency comb interval measurements," J. Opt. Soc. Am. B **23**(10), 2200–2208 (2006).
32. J. L. Hall, and C. J. Borde, "Shift and broadening of saturated absorption resonances due to curvature of laser wave fronts," Appl. Phys. Lett. **29**(12), 788–790 (1976).
33. S. E. Park, H. S. Lee, T. Y. Kwon, and H. Cho, "Dispersion-like signals in velocity-selective saturated-absorption spectroscopy," Opt. Commun. **192**(1-2), 49–55 (2001).
34. E. A. J. Marcatili, and R. A. Schmeltzer, "Hollow Metallic and Dielectric Wave-guides for Long Distance Optical Transmission and Lasers," Bell Syst. Tech. J. •••, 1783–1809 (1964).

1. Introduction

Overtone transitions in acetylene near 1.5 µm have been precisely measured using saturated absorption spectroscopy in power build-up cavities [1–6] and vapor cells [7], and form a frequency standard with an accuracy of ± 2 kHz. High optical stability is also exhibited, exceeding that of a quartz oscillator. However, these features are realized in free space configurations that establish long interaction lengths and high saturation intensities. Fiber-based high-accuracy spectroscopy would be of benefit to portable frequency standards [8] and trace gas analysis. Hollow-core photonic crystal fibers (HC-PCF's) confine both gas and light in a relatively small core, allowing for the realization of narrow sub-Doppler features [9–13].

Furthermore, HC-PCF's offer a portable and potentially more robust medium in which to realize saturated absorption with sufficient stability and accuracy for a frequency reference [14]. More importantly, HC-PCF's have sufficiently low loss to facilitate nonlinear optical interactions with extremely low power levels [15,16]. On the other hand, the tight transverse confinement of the guided laser beam in HC-PCF's sets a limit on the linewidths of saturated absorption features, which are dominated by transit time broadening (i.e. the time molecules coherently interact with the laser field before colliding with the core walls). Linewidths on the order of 40 MHz full width half maximum (FWHM) have been observed in commercially available 7-cell HC-PCF's [17] and methods have been shown experimentally to further reduce this linewidth to 15 MHz FWHM by slow molecule selection [11]. Larger core HC-PCF has also been shown to reduce the linewidth through increased molecular transit time [18]. Kagome HC-PCF [19], which was used to observe narrow electromagnetically-induced transparency (EIT) features in Rb [13], possesses a lattice with a much larger unit cell and consequently offers larger core sizes with higher loss per unit length (~1 dB/m) than the photonic bandgap HC-PCF. One important advantage of kagome fiber over HC-PCF is that it does not suffer from the effect of surface modes which can cause an oscillatory background in the transmission spectrum, which in turn degrades the contrast. This arises due to the intrinsic guidance mechanism in this class of HC-PCF whereby the coupling between hollow-core modes and silica cladding modes is dramatically reduced [19].

Here we observe saturated absorption spectra in 19-cell kagome fiber with a maximum core diameter of 68 μm, and investigate the dependence on pressure and power of the P(13) v_1 + v_3 transition in $^{12}C_2H_2$. Additionally, frequency modulation (FM) spectroscopy [20–22] is incorporated into the saturated absorption spectroscopy setup to stabilize the laser frequency to the P(13) line. The accuracy and short-term instability of the frequency standard are then characterized by analysis of an optical heterodyne beat with a frequency comb referenced to a GPS-disciplined Rb oscillator. The accuracy (± 9.3 kHz) and instability (< 1.2×10^{-11} in 1 s) of this reference are compared with those of power build-up cavities and vapor cells, and reveal the suitability of the kagome fiber for sub-Doppler spectroscopy. Finally, we discuss prospects and limitations on the ultimate accuracy of kagome-based portable frequency references.

2. Saturated absorption spectroscopy inside kagome HC-PCF

Saturated absorption spectroscopy (SAS) is used to characterize sub-Doppler features in acetylene-filled kagome fiber. The schematic for this experiment is shown in Fig. 1(a), and a similar setup is explained in Ref [18]. The kagome fiber lies between two vacuum chambers, which are evacuated for at least 1 hour to ~20 mtorr before the acetylene is introduced at a given pressure for about 1 hour to establish equilibrium. A narrow linewidth (~500 Hz at 100 ms) continuous-wave (CW) fiber laser, purchased from Orbitz Lightwave, Inc., has a tuning range of 10 GHz allowing observation of the P(13) v_1 + v_3 ro-vibrational transition in $^{12}C_2H_2$. As shown in Fig. 1(a), the CW fiber laser seeds an IPG Photonics erbium doped fiber amplifier (EDFA) which creates the pump beam and the much weaker probe beam. The probe beam is frequency shifted by an acousto-optic modulator (AOM) so that any interference between the pump and probe beams occurs at the AOM modulation frequency of ~55 MHz. The pump and probe beams are both coupled to free-space, through wedged vacuum windows, and then into the ends of the large core kagome HC-PCF (48 μm × 68 μm irregular hexagon core shown in Fig. 1(a)) so that they counter-propagate down the length of the fiber. Polarization optics make the probe beam polarization orthogonal to the pump beam at the polarizing beam splitter (PBS) after exiting the kagome fiber, where a photodetector (PD) is used to record the probe transmission. Applying a ramp voltage to the fiber laser's piezo-electric transducer (PZT) linearly scans the laser frequency, shown in Fig. 1(b). A small portion of the probe light is sent through a fiber ring cavity (FRC), which is a fiber coupler with an output port connected to the secondary input. The free spectral range (FSR) of the

cavity was measured to a fractional uncertainty of 0.02% by tuning the sidebands of an electro-optic modulator (EOM) to overlap with the resonances of adjacent cavity modes.
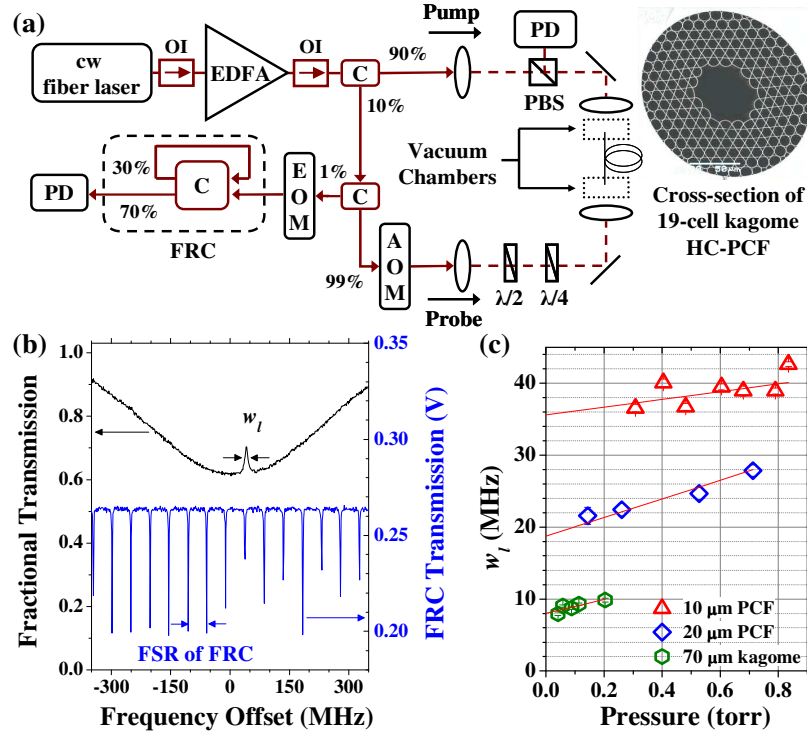
Fig. 1. (a) Schematic of the saturated absorption spectroscopy setup. Solid lines indicate optical fiber, and dotted lines indicate free-space paths. Shown are fiber optical isolators (OI), fiber couplers (C), a polarizing beam splitter (PBS), photo-detectors (PD), and a cross-section of the 19-cell kagome HC-PCF [19]. (b) (left axis) Normalized fractional transmission of a 4.1 m long HC-PCF near the P(13) transition for a pump laser power of 32 mW exiting the fiber, while the laser frequency was scanned at 1.2 GHz/sec. (right axis) The output from the FRC with a FSR of 48.01 ± 0.01 MHz. (c) Sub-Doppler FWHM w_l versus pressure with fit lines extrapolated to zero pressure of the P(11) transition inside the 10 μm (triangles) and 20 μm (diamonds) HC-PCF (previously reported in Ref [18].), and of the P(13) transition inside the kagome fiber data (hexagons). The lengths of each fiber in order of increasing core size are 0.9 m, 0.8 m, and 4.1 m, while the pump powers exiting the three fibers are 30 mW, 29 mW, and 32 mW, respectively. Error bars from a chi-squared fitting routine are smaller than the symbol size.

Spectra were recorded at several different acetylene pressures at an off-resonant optical pump power of 32 mW exiting the kagome fiber. The natural logarithm of the recorded transmission was taken to convert this data into the dimensionless product of absorbance and length as described in Ref [18]. The FWHM of the sub-Doppler absorbance features, w_l, are plotted in Fig. 1(c) as a function of pressure with previous data from 10 and 20 μm HC-PCF's [18]. These data also exhibit ~10 MHz/torr pressure broadening, in agreement with measurements at higher pressures [8]. The zero-pressure intercept of the linewidths (36 MHz, 19 MHz, and 8 MHz) shows an inverse relation to the three different core size PCF's (10 μm, 20 μm, and 50-70 μm) and is due to the increasing molecular transit time. It should be noted that kagome fiber has a loss value of ~1 dB/m at 1530 nm [19], which is considerably higher than the loss of the smaller core HC-PCF's that use photonic bandgap guidance [17]. Thus the linewidths should be more power-broadened in the kagome fiber than in small core HC-PCF's for similar powers exiting the fiber. Even so, the 8 MHz FWHM linewidths in Fig. 1(c) are

the smallest yet observed using SAS of acetylene inside photonic crystal fiber. Additional linewidth narrowing could be observed using a fiber with a larger core diameter, or through the slow molecule selection technique reported in Ref [11].

3. Stability of the acetylene-stabilized laser

CW laser stabilization is achieved by employing an FM spectroscopy technique capable of detecting Doppler-free dispersion signals. The optical and electrical schematics for CW laser stabilization are shown in Fig. 2, and contain slight modifications of the optical setup in Fig. 1(a). The probe beam passes through a fiber EOM (General Photonics LiNbO$_3$ phase modulator) to generate FM sidebands (f_{FM} = 22 MHz) where 50% of the carrier power is shifted into the first order sidebands. Also, amplitude modulation (f_{AM} = 900 kHz) of the pump is used to reduce offsets due to the Doppler-broadened background. A high bandwidth PD (New Focus 1811-FC) is used to detect the modulation frequencies and requires fiber coupling via the PD fiber. The PD signal is filtered, amplified, and mixed at both f_{FM} and f_{AM} to observe a Doppler-free absorption signal shown at the bottom left corner of Fig. 2. This dispersion feature with odd-symmetry is used as the input error signal to servo the CW fiber laser to the P(13) transition of the $v_1 + v_3$ ro-vibrational transition in $^{12}C_2H_2$.
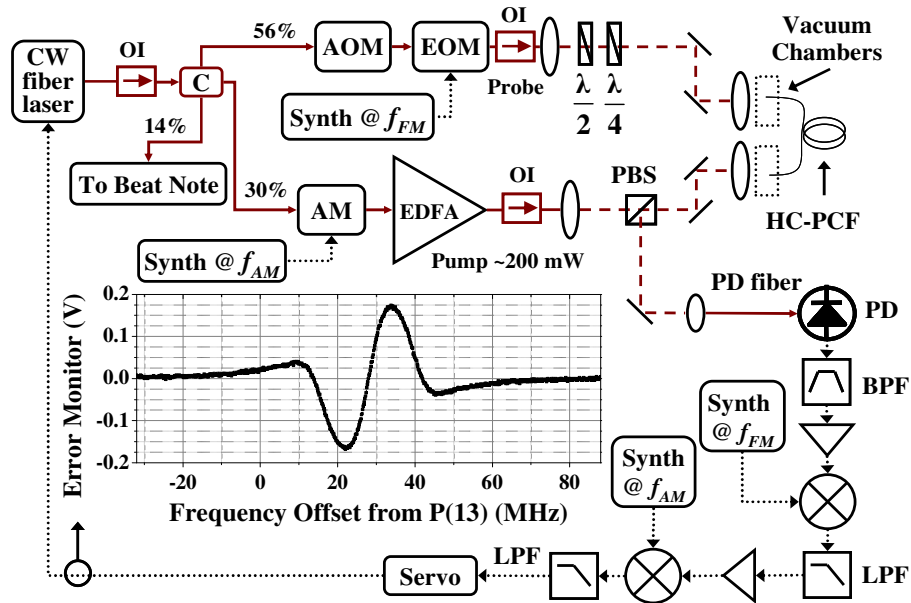
Fig. 2. Optical and electrical schematic for stabilizing a CW laser to $^{12}C_2H_2$ inside kagome HC-PCF. An EOM phase modulates the probe beam that is detected by the PD, whose electrical signal is band pass filtered (BPF) and amplified before being mixed with a phase adjustable synthesizer (Synth). An AM amplitude modulates the pump beam, so the electrical signal is again filtered, amplified, and mixed. The resulting signal is then sent to a servo that feeds back to the fiber laser's PZT after being filtered with a 60 kHz low pass filter (LPF) and is shown in the lower left corner.

The CW reference's optical frequency stability is characterized by heterodyning the laser with a self-starting carbon nanotube fiber laser (CNFL) frequency comb [23] shown in Fig. 3(a). The CNFL has a typical ring configuration where the carbon nanotubes act as a saturable absorber inside the cavity, and are placed on the end of an optical connector of a PZT fiber stretcher which is used to control the cavity length. The laser is followed by a parabolic pulse fiber amplifier which uses a low-dispersion-slope HC-PCF [24] before a supercontinuum is generated in the highly nonlinear fiber. Both the repetition frequency (f_{rep}) of 167 MHz and the carrier-envelope offset frequency (f_0) of 60 MHz are detected and stabilized to a Precision

Test Systems (model GPS10RB) GPS-disciplined Rb oscillator (Rb/GPS) [25]. These fundamental comb parameters are then counted with HP53132A 12-digit frequency counters, and the RF heterodyne signal (f_{beat}) is counted with an HP53131A 10-digit frequency counter as shown in Fig. 3(b).
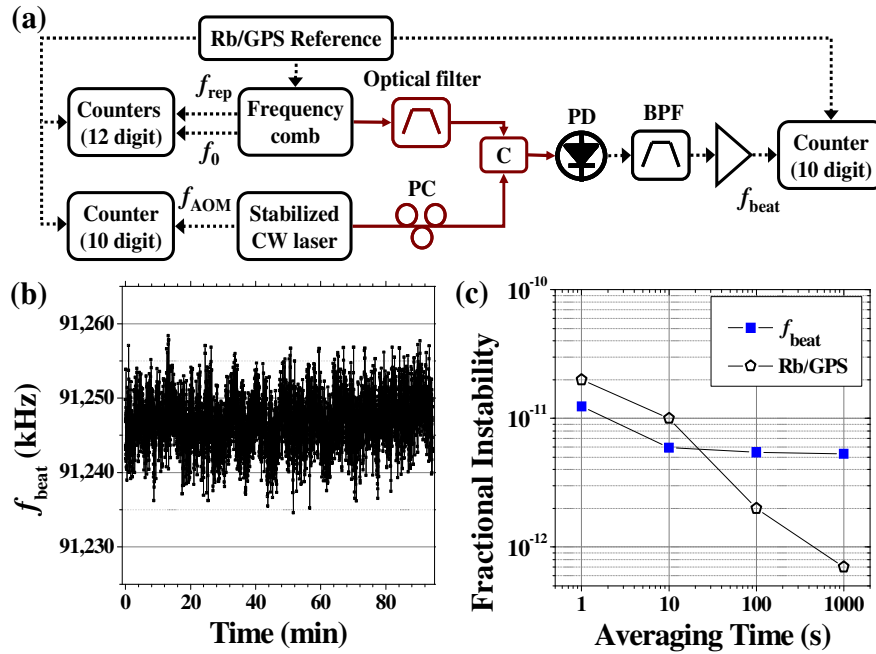
Fig. 3. (a) Optical and electrical schematic for the heterodyne beat between a stabilized frequency comb and a CW laser stabilized to $^{12}C_2H_2$ inside kagome HC-PCF. The frequency counters used to record the various RF signals had either 10 digit (HP53131A) or 12 digit resolution (HP53132A). Shown is a fiber polarization controller (PC). (b) Frequency of the beat between the HC-PCF acetylene-stabilized laser and the CNFL frequency comb vs. time, recorded at a 1 s gate time using a counter. Oscillations with a period of ~10 minutes correlate to air-conditioner cooling cycles. (c) Optical fractional frequency instability vs. averaging time for f_{beat} (filled squares) and the GPS disciplined Rb oscillator (open pentagons). A triangle deviation, similar to an Allan deviation, was calculated for f_{beat}.

At 1500 nm, the dominant source of instability in the CNFL comb is f_{rep}. The triangle deviation, an estimate of the Allan deviation that is distorted by the interpolation of our frequency counters [26], is calculated for f_{beat} (σ_{beat}) and f_{rep} (σ_{rep}) to determine the heterodyne instability and the comb's in-loop instability. Fractional frequency instabilities in the optical domain are plotted in Fig. 3(c) for the beat frequency (squares) and the Rb/GPS (pentagons). The instabilities given by the Rb/GPS manual are typical values, and have not been measured for the particular unit used in this experiment. The CNFL comb's instability is limited by the Rb/GPS reference, and therefore dominates the beat frequency's instability at short gate times. The beat sets an upper limit on the instability of the HC-PCF acetylene-stabilized laser, which is within an order of magnitude of other acetylene-based frequency references in power build-up cavities and gas cells at 1 s averaging times [4,5,7]. The higher instability is attributed to the broader sub-Doppler linewidths observed in HC-PCF (~8 MHz) relative to the linewidths of free-space configurations used in the previously mentioned experiments (~1 MHz). The optimum potential relative instability of this reference was calculated to be $1.0 \times 10^{-12} \tau^{-\frac{1}{2}}$, where τ is the averaging time, from an estimated noise density of 1.5×10^{-12} $(Hz)^{-\frac{1}{2}}$ by comparing the off-resonant noise (9 mV_{pk-pk}) to the slope of the feature (22 kHz/mV) within the 60 kHz bandwidth and assuming white frequency noise (from Fig. 2) [27]. Deviations

from the expected $\tau^{-\frac{1}{2}}$ behavior for $\tau > 10$ s are attributed to the air-conditioner cycles depicted in Fig. 3(b).

4. Absolute frequency of the acetylene-stabilized laser

A free-space prism-based Cr:forsterite (Cr:f) laser frequency comb [28] that allows for large (~kHz) changes in f_{rep} (~113 MHz) is used to characterize the absolute frequency of this optical reference. The optical reference's frequency (f_{laser}) and the nearest comb tooth's frequency (f_n) are given by the equations

$$f_{laser} = f_x + \tfrac{1}{2} f_{AOM}, \tag{1}$$

$$f_{laser} \pm |f_{beat}| = f_n, \quad \text{and} \tag{2}$$

$$f_n = n \cdot f_{rep} \pm |f_0|, \tag{3}$$

where f_x is the experimental frequency of the P(13) $v_1 + v_3$ ro-vibrational transition in $^{12}C_2H_2$, f_{AOM} is the frequency of the probe beam's AOM, f_n is the frequency of the nearest comb tooth, and n is the integer mode number of this nearest tooth. The signs of f_{beat} and f_0 are ambiguous due to the mixing process, and are determined by changing the frequency lock point of both f_{rep} and f_0 while observing f_{beat}. The absolute frequency of the reference is calculated by using a technique similar to Ref [29]. The repetition frequency is changed such that f_{beat} represents the beat between the optical reference and the $n + m$[th] comb tooth, where the integer m can be directly observed. Comparing Eqs. (1-3) for two different values of f_{rep} allows for the solution of n in terms of f_{beat}, f_{AOM}, $f_{rep,1}$, $f_{rep,2}$, f_0, and m. Assuming that the instabilities of these parameters are uncorrelated, the uncertainty of n (Δn) is given by

$$\Delta n = \frac{\sqrt{2\left((\Delta f_0)^2 + (\Delta f_{beat})^2 + (\tfrac{1}{2}\Delta f_{AOM,1})^2\right) + \left(n^2 + (n+m)^2\right)(\Delta f_{rep})^2}}{(f_{rep,2} - f_{rep,1})}, \tag{4}$$

where $f_{rep,1}$ and $f_{rep,2}$ are the initial and final repetition frequencies, respectively, and the Δf's indicate the uncertainty on each frequency. Typical uncertainties of the frequencies after averaging for 30 minutes are estimated by their standard deviations, and are: $\Delta f_0 \approx 1 \text{Hz}$, $\Delta f_{beat} \approx 20 \text{kHz}$, $\Delta f_{AOM} \approx 1 \text{kHz}$, and $\Delta f_{rep} \approx 1 \text{mHz}$. To know n to the nearest integer ($\Delta n < 1$) in Eq. (4), values of $m > 900$ would be necessary, but keeping the comb locked over such a large change is challenging and time-consuming. Therefore, measurements are made with $m \approx 10$ at two different values of f_{rep} separated by up to 200 kHz. Each measurement therefore had a $\Delta n \approx 40$, and f_{laser} was calculated for the two data sets for all possible values of n. When compared, 6 measurements agreed at a single value of f_{laser} to within 100 kHz. Thus the mode number of the nearest tooth was resolved. However, higher accuracy of $\pm$ 20 kHz was expected on the ~10 MHz wide feature in view of the $\pm$ 2 kHz accuracy achieved with a ~1 MHz wide sub-Doppler feature in power build-up cavities [30,31] or vapor cells [7].

   The cause of the 100 kHz inaccuracy was discovered to be the laser alignment into the fiber. When the pump or probe beam alignment into the fiber was changed such that the power through the fiber was reduced by a factor of two, the frequency lock point of the acetylene-stabilized laser experienced ~100 kHz shifts. In contrast, no shifts were observed when the power was reduced by a factor of two while alignment was preserved. Similar changes in alignment into the PD fiber (middle right of Fig. 2), which was initially single mode fiber (SMF-28), demonstrated shifts on the order of 100's of kHz. Now that the PD fiber is switched to multi-mode fiber (MMF), the frequency dependence on the pump and probe alignment is smaller by roughly a factor of two, while the frequency dependence of the coupling into the PD fiber remains on the order of 100 kHz. More importantly, the frequency

shift became centered about the optimum alignment for peak power. When the system's peak power is optimized through the kagome and PD fiber, the frequency of the lock point is repeatable to ± 20 kHz. No shifts greater than 10 kHz are observed when servo polarity, FM phase polarity, and AM phase polarity are reversed.

The dependence of the laser frequency on pump and probe alignment suggests that different spatial modes inside the kagome fiber experience different phase shifts. The alignment sensitivity is mitigated with a multi-mode fiber before the PD, suggesting that the multi-mode PD fiber collects more of the higher order modes simultaneously, allowing the various shifts from various modes to cancel more completely. It is reasonable that different spatial modes experience different shifts. Shifts in saturated absorption signals are known to arise from wave front curvature [32] and in angular beam deviations [33]. If one considers the pump (or probe) beam to be in the fundamental mode, and some of the power of the probe (or pump) beam to be in the next higher mode, then a series of crossings between the pump and probe occur. The effective angle between the guided modes can be calculated from the difference in the propagation constant β, which in the case of kagome HC-PCF can be approximated to that of a capillary waveguide:

$$\beta_{nm} = k\left(1 - 2\left(\frac{u_{nm}}{k \cdot d}\right)^2\right). \tag{5}$$

In Eq. (5), k is the wave vector amplitude and d is the fiber core diameter. The subscripts are the guided mode indices and u_{nm} is the mth root of $J_{n-1}(u_{nm}) = 0$ [34]. During a misalignment, the coupled beam can partially "hop" from the fundamental mode HE_{11} to the first higher order mode set ($TE_{01} + HE_{21}$). The propagation mismatch between the two sets of modes is $\Delta\beta = \left(\lambda/\pi d^2\right)\left(u_{11}^2 - u_{21}^2\right) = 2.8\left(\lambda/d^2\right)$. From a simple ray picture the phase mismatch between these modes corresponds to a mismatch of their wave fronts of $\Delta\theta = \left(\lambda/\pi d\right)\left(u_{11} - u_{21}\right) = 0.45\left(\lambda/d\right)$ rad. If the beams were to cross in free-space at this angle at one end of an absorption cell, a frequency shift $\Delta f = (v_{thermal}/\lambda)\sin(\theta/2) = 2\,MHz$ would be observed [33]. We postulate that many crossings occur in the kagome fiber, causing the shifts to generally cancel out. Additionally, the pump and probe beams are likely to be exciting different distributions of higher order modes, which could account for these residual shifts. In a fused, vibrationally isolated photonic crystal microcell (i.e. a gas-filled HC-PCF spliced to a conventional optical fiber) [9], such random shifts are likely to be reduced, although a permanent shift may result. Further investigation is ongoing.

To fully characterize the gas-filled fiber frequency accuracy, a series of measurements were made under a variety of acetylene pressures. The beat between the stabilized CW laser and the convenient CNFL comb was counted for over 1000 s at 1 s gate time and averaged. The absolute frequency of the acetylene-stabilized laser (f_{laser}) was already measured to within 100 kHz with the Cr:f laser, which allowed for the determination of n (which must be an integer) in subsequent measurements from Eqs. (1-3). Figure 4 plots the frequency of the reference with the AOM shift removed (f_x) versus acetylene pressure inside the kagome fiber, and each data point indicates an independent realignment of the SAS setup. A linear fit through these data gives a zero-pressure intercept of (195,580,979,379.6 ± 5.6) kHz with a slope of (−369 ± 48) kHz/torr.

Systematic shifts and uncertainties in the absolute frequency arise due to residual gas pressure, fiber alignment, pump power, and attenuation in the fiber. The residual pressure in the chamber was ~20 mtorr, which implies a 7.4 kHz uncertainty using the measured pressure shift of 369 kHz/torr. This pressure shift has an error of ± 61 kHz/torr when a 10% pressure calibration error is included, and is near the value of (−270 ± 30) kHz/torr (2 σ error) recorded at pressures of ~50 torr in Ref [8]. Alignment shifts were also considered, and were

effectively transformed into statistical error by repeated alignment of the system. A frequency shift of −1.6 kHz was calculated by multiplying a previously reported power shift of −11.4 Hz/mW (Ref [1].) by 144 mW of average pump power, accounting for attenuation down the length of the fiber.
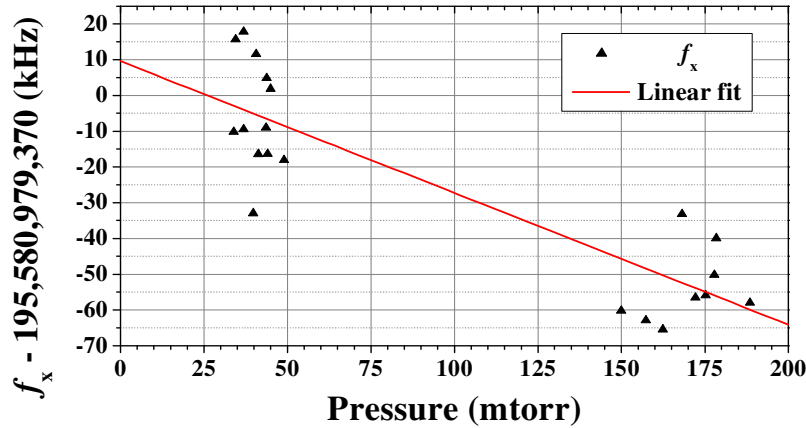
Fig. 4. Absolute frequency of the acetylene-stabilized laser versus acetylene pressure inside the 4.1 m kagome fiber with a linear fit line. Each data point indicates an independent alignment to avoid frequency offsets due to free-space coupling into the kagome fiber. The linear fit gives a zero-pressure intercept of (195,580,979,379.6 ± 5.6) kHz and a slope of (−369 ± 48) kHz/torr.

The P(13) frequency measured in this work is listed alongside an error budget in Table 1 with values from Refs [30,31]. It should be noted that the total error bar on this measurement is within an order of magnitude of those from similar experiments using SAS in power build-up cavities and vapor cells with ~1 MHz features [1,3–5,7,30,31]. The measured value, when corrected for pressure and power shifts, is (195,580,979,378.0 ± 9.3) kHz, which agrees with previously measured values within the uncertainty. From this agreement, we conclude that fiber-induced shifts such as those caused by wall collisions do not arise at the 10 kHz level. Thus the gas-filled kagome fiber is a suitable medium for precision spectroscopy.

Table 1. Mean $^{12}C_2H_2$ $v_1 + v_3$ P(13) frequency and error budget for this work and for referenced work [**30,31**].

| | Uncertainty (kHz) | | | | Mean P(13) value (kHz) |
	Statistical[†]	Pressure[‡]	Power[‡]	Total	
This work	5.6	7.4	0.6	9.3	195,580,979,378.0
Ref [31]. *	-	-	-	3.7	195,580,979,370.4
Ref [30].	2.0	10.0	-	10.2	195,580,979,371.1

[†] Type A uncertainty
[‡] Type B uncertainty
* individual uncertainties were not listed for the P(13) line

5. Summary

Saturated absorption spectroscopy was carried out inside acetylene-filled kagome fiber and 8 MHz FWHM linewidths were observed, which are the narrowest to date in fiber. FM spectroscopy was then performed to stabilize a narrow linewidth fiber laser to the P(13) $v_1 + v_3$ overtone transition in $^{12}C_2H_2$ with an in-loop signal-to-noise ratio of 34 in a bandwidth of 60 kHz. A heterodyne beat note measurement between this system and a CNFL frequency comb determined the relative short-term instability of the system to be less than 1.2×10^{-11} (or

2.3 kHz) at a 1 s gate time, limited by the GPS-disciplined Rb oscillator used to reference the frequency comb.

The P(13) absolute frequency measured in this hollow fiber system agrees with previous measurements, and the resulting uncertainty of 9.3 kHz is the lowest yet reported inside a fiber. Thus, gas-filled kagome fiber is suitable for precision spectroscopy. These measurements were made by comparing to both a Cr:forsterite comb with tunable f_{rep} and a CNFL comb. Significant sensitivity of the locking point to alignment into the fiber was observed. Lower uncertainties may be achieved if the linewidth can be further reduced without increasing the alignment sensitivity. Furthermore, sealed fiber microcells made of kagome HC-PCF may exhibit lower uncertainty as a reference due to the fusion of solid core fibers fixing the alignment into the cell, especially when vibrationally isolated.

Acknowledgements